THE OFFICIAL MAGAZINE OF THE OCEANOGRAPHY SOCIETY

Oceanography

CITATION

Henderikx Freitas, F., G.S. Saldías, M. Goñi, R.K. Shearman, and A.E. White. 2018. Temporal and spatial dynamics of physical and biological properties along the Endurance Array of the California Current ecosystem. *Oceanography* 31(1):80–89, https://doi.org/10.5670/oceanog.2018.113.

DOI

https://doi.org/10.5670/oceanog.2018.113

Temporal and Spatial Dynamics of Physical and Biological Properties along the Endurance Array of the California Current Ecosystem

By Fernanda Henderikx Freitas, Gonzalo S. Saldías, Miguel Goñi, R. Kipp Shearman, and Angelicque E. White

ABSTRACT. The coastal margin of the Pacific Northwest of the United States is a highly dynamic and productive region. Here, we use satellite, high-frequency mooring, and glider estimates of biologically relevant physical and optical variables to characterize seasonal patterns and latitudinal and cross-shore gradients in particle concentrations between the Washington and Oregon shelves. Consistent with prior research, we find that the Columbia River exerts a strong seasonal influence on the Washington shelf, but smaller coastal rivers and resuspension processes also appear important in determining particle distributions nearshore during winter across the full study region. We find fluorescence-based measurements of chlorophyll to be similar in magnitude across the two shelves over the time period examined, although the much weaker wind stresses off Washington indicate that processes other than upwelling are important determinants of chlorophyll changes in those areas, as previously suggested. These in situ observations contrast with the overall differences observed from satellite data, which consistently show higher chlorophyll concentrations off the Washington coast. This research suggests that latitudinal differences in chromophoric dissolved organic matter may be a partial explanation for perceived trends in satellite-derived chlorophyll. The observations presented are nascent; maturation of temporal and spatial coverage of OOI data sets will be necessary to more conclusively link physical forcing and biogeochemical responses.

OOI technicians from Oregon State University and the crew of R/V *Atlantis* deploying the Newport Line moorings in 2016. *Photo credit: Katie Watkins-Brandt*

INTRODUCTION

Embedded within the California Current System, the coastal ocean along the Pacific Northwest (PNW) of the continental United States has recently become highly instrumented with the installation of an array of moored and autonomous assets via the National Science Foundation-supported Ocean Observatories Initiative (OOI). The oceanography of this area is complex. Strong temporal and spatial variability in the physics and biogeochemistry of the upper water column is largely the result of wind-driven upwelling and downwelling processes, as well as the freshwater influence of the fourth largest river in North America and other numerous small mountainous rivers. Monitoring changes in the ecological properties of these heterogeneous regions is challenging and requires both synoptic surveys and high-resolution Eulerian time series.

Large-scale upwelling along ocean margins occurs mainly in eastern boundary regimes (e.g., Peru/Chile, Southeast Atlantic, PNW) and is a highly seasonal phenomenon driven by shifts in wind strength and direction. In the PNW, prevailing northerly winds lead to intense upwelling periods when cold, dense, and nutrient-rich waters advected onto the continental shelf reach the euphotic zone (e.g., Huyer, 1983), resulting in enhanced phytoplankton production (e.g., Dickson and Wheeler, 1995) and the formation of biogenic particles (e.g., Wetz and Wheeler, 2003). Wind forcing also drives fluctuations in surface currents, water properties, and sea level, with typical scales of variability on the order of three to 10 days (Hickey and Banas, 2003). Additionally, upwelling-favorable winds drive cross-shelf transport that actively pushes the freshwater plume of the Columbia River southward and offshore of the Oregon shelf in the spring and summer months (Barnes et al., 1972; Hickey et al., 2005; Saldías et al., 2016).

Much less is known about the biogeochemistry of non-upwelling periods, even though these conditions are sustained throughout much of the year. For example, downwelling-favorable winds and moisture-laden storms prevail along the PNW in fall and winter months, which leads to large fluvial inputs of biogeochemically relevant, land-derived constituents to the coastal ocean, including freshwater (i.e., buoyancy), dissolved inorganic nutrients, and dissolved and particulate organic matter (e.g., Wheatcroft et al., 2010; Goñi et al., 2013). During these periods, the colder waters of the Columbia River are diverted northward over the Washington shelf and slope, altering regional current patterns (Hickey et al., 1998).

Productivity in the PNW has traditionally been assessed from shipboard surveys and satellite data. Studies comparing the productivity patterns of the Washington and Oregon shelves have concluded that absolute chlorophyll (chl) concentrations, a proxy for productivity, as well as the cross-shelf extent of chl signals, are seasonally larger for the Washington shelf despite significantly weaker upwelling winds relative to Oregon (Hickey and Banas, 2003, 2008; Davis et al., 2014). Ware and Thomson (2005) reported similar patterns of increased concentrations of chl, zooplankton, and fish to the north of the California Current System. In these studies, the seeming paradox was attributed to key geographical differences between the two locations, namely (1) the continental shelf is broader in Washington, thus potentially leading to increased residence times for nutrient and phytoplankton-rich waters in the region, (2) the Columbia River, which flows north into the Washington shelf during much of the year, is a potential source of limiting nutrients including iron and silicate, (3) proximity to the Strait of Juan de Fuca in British Columbia, Canada, likely allows for the advection of nutrient-rich waters onto the Washington shelf, and (4) the larger number of submarine canyons off the Washington shelf potentially allows for deeper, nutrient-rich waters to reach areas closer to the surface over the seasons and sustain productivity during weak upwelling periods.

In the following, we summarize long-term satellite estimates of particle distributions for the Washington and Oregon shelves, and raise the importance of considering the contribution of chromophoric dissolved organic matter (CDOM) in the interpretation of productivity patterns from satellite data. Then, we describe latitudinal gradients in temperature, salinity, pigment fluorescence, CDOM, and particle backscattering from high-frequency OOI observations during upwelling and downwelling periods of 2015 and 2016. Finally, we discuss the potential roles of wind-driven upwelling, resuspension processes, and riverine discharge in driving particle distributions across the Washington and Oregon shelves.

METHODS AND DATA SOURCES

OOI Endurance Array

The OOI Endurance Array (http://oceanobservatories.org/array/coastal-endurance) provides observations of cross-shelf and along-shelf variability in oceanographic properties off the Oregon and Washington coasts via a set of moorings and autonomous glider surveys (see map in Smith et al., 2018, in this issue). Two cross-shelf moored array lines, the Oregon (OR; Newport Line, ~44.6°N, inshore of 125°W) and Washington (WA; Grays Harbor Line, ~47°N, inshore of 125°W) lines each include inshore, mid-shelf, and offshore moorings at bottom depths of approximately 25, 80, and 600 m. In this work we used in vivo fluorescence-based estimates of chlorophyll (chl, mg m^{-3}) and fluorescent-based CDOM (370 ± 20 nm / 460 ± 120 nm excitation/emission wavelengths, ppb), volume scattering coefficients at 700 nm (β (124°), m^{-1} sr^{-1}), water temperature, and salinity data sets from the OR and WA OOI surface mooring sensor packages, nominally sampled at 7 m depth as determined by the OOI mooring design. All available recovered and telemetered data from the January 2015 to March 2017 data period were acquired to improve temporal coverage; no QA/QC flags had

been previously applied to these data. Instances of discrepancies between recovered and telemetered data were observed, in which case the recovered data sets were selected. Personal communication with OOI data managers indicated that these discrepancies were due to "time-of-day" telemetry errors.

Chlorophyll and CDOM data were obtained in scaled units based on OOI pre-deployment calibration coefficients, and only nighttime chl data are used in the analysis to avoid the effects of quenching of chl fluorescence during daylight hours (Müller et al., 2001). Volume scattering coefficients were converted to particulate backscattering coefficients (b_{bp}, m^{-1}) using the relationship $b_{bp} = 2\pi\chi\beta_p(\theta)$, where χ is a dimensionless factor equal to 1.076 based on Sullivan et al. (2013), and the particulate volume scattering β_p is obtained by subtracting the volume scattering of seawater of Zhang et al. (2009) from β. Particulate backscattering is considered a proxy for suspended particles, including phytoplankton, detritus, and sediments (Jonasz and Fournier, 2011). The CDOM instrument configuration is specific for estimation of humic-like dissolved organic matter, and thus is a proxy for land-derived materials transported by rivers (Coble, 1996). Data presented here as daily averages were smoothed using a one-hour moving average filter on log-transformed observations to reduce the effect of high-frequency variability. The minimum values of chl, b_{bp}, and CDOM per mooring were subtracted from each time series to facilitate mooring-to-mooring comparisons, given that OOI biological sensors are not intercalibrated.

Despite the long-term sampling efforts, several sections of data were excluded from the analysis due to low quality of the retrieved outputs. These included raw volume scattering count data between October 2014 and April 2015 for both inshore moorings that were characterized by a repetitive pattern of progressive signal increase up to the upper limit of detection, followed by abrupt drops to zero values. Similar issues (e.g., maxed-out values possibly associated with biofouling) affected several sections of data from these moorings between January and May 2016. Additionally, data density is often more complete for the OR line than the WA time series, which yields large gaps in the comparative data set. For example, only 66 days of data are available for the offshore WA mooring in 2015, compared to 268 days for the offshore OR mooring.

Nearly coincident glider observations from the WA (glider/deployments g386/2, g384/3, and g312/4) and OR (g384/1, g320/2, and g382/2) long Endurance Lines (sampling between 128°W and 125°W) were obtained for the period 2015–2016, totaling about 40 days of data at each line. From these data, we calculated freshwater content (FWC; m), which represents the thickness of freshwater in the water column, as follows:

$$FWC = \int_{-d}^{0} \frac{(S_0 - S)}{S_0}\, dz, \qquad (1)$$

where S is salinity, S_0 is the reference salinity of 32.5 for the Columbia River plume (Barnes et al., 1972), and d is the plume thickness according to the depth of S_0.

Additional glider-derived optical data (chl, CDOM, and b_{bp}) from the short Endurance Lines (sampling between 125°W and 124.3°W) off WA and OR were obtained (g326/1, g247/4, g381/1 and g311/1). Mission configurations consisted of repetitive cross-shore transects, with each deployment lasting between one and two months. Few simultaneous glider deployments were available for WA and OR, or at the times of moored observations. Thus, mean cross-shore sections per deployment were acquired as examples of cross-shore distributions of bio-optical properties during different times of the year at the two lines. A deep offset correction was applied to all glider optical data in order to improve comparisons between data from different gliders (Schmechtig et al., 2014).

Wind stress, significant wave heights, and river discharge measurements were used to inform potential controls on the observed physical and bio-optical observations. Wind and wave data were obtained from NOAA's National Data Buoy Center (NDBC) buoys 46041 and 46050 (http://www.ndbc.noaa.gov). Hourly Columbia River discharge data were obtained from US Geological Survey gauge 14105700 (https://nwis.waterdata.usgs.gov). Monthly discharge totals for 21 small mountainous rivers along the OR-WA coastline were obtained from USGS gauges (Figure 1a). All correlation coefficients (r) shown in this study are considered significant if within the 95% confidence interval.

Satellite Observations of Phytoplankton and Particle Distributions

Monthly satellite retrievals of chlorophyll (chl_{sat}), absorption coefficients of non-algal materials and CDOM at 443 nm ($a_{cdom}(443)$), and remote sensing reflectances at 555 nm (R_{rs} (555)) from 2003 to 2016 were obtained from NASA MODIS Aqua Level 3 data products (https://oceancolor.gsfc.nasa.gov). Here, chl_{sat} (NASA's OCx algorithm) is considered a proxy for the presence of phytoplankton (e.g., Cullen, 1982). As a proxy for the concentration of CDOM in coastal waters, $a_{cdom}(443)$ was estimated from the Garver-Siegel-Maritorena bio-optical algorithm (Maritorena et al., 2002). $R_{rs}(555)$ is, to first order, a proxy for the influence of low-salinity and sediment-rich river plumes in the coastal PNW (e.g., Thomas and Weatherbee, 2006; Saldías et al., 2016). $R_{rs}(555)$ is correlated with chl_{sat} and presumably plankton biomass in clear oceanic waters not influenced by strong land-ocean interactions.

RESULTS AND DISCUSSION

Latitudinal Gradients in Satellite and Glider Properties and the Impact of Riverine Inputs

The variability in the magnitude and seasonality of river discharge along the Washington-Oregon margin is illustrated in Figure 1a. The dominant and year-round

influence of the Columbia River is clear, with peak discharge in winter and spring as a result of precipitation and melt of the continental snow pack. Columbia River flows are largely regulated by dams, which dampen seasonal discharges and keep summer flows artificially high because of releases from hydroelectric operations. The smaller mountainous rivers that line the PNW margin show wintertime peaks in discharge following seasonal precipitation patterns, with very low flows in the summer. Between November and March, the combined discharge of the 21 gauged small mountainous rivers equals about 30%–50% of the discharge of the Columbia River over the same period, while in the summer months the small rivers are equivalent to less than 10% of the Columbia River discharge. The geographical locations of the WA and OR lines relative to major river inputs help explain some of the patterns discussed in this study. For instance, the WA line is under direct influence of the Columbia River, while the OR line is influenced by a few small mountainous rivers (e.g., Alsea and Yaquina) and is considerably far from the mouths of more important rivers to the south (e.g., Umpqua and Rogue).

Temporal variability of $R_{rs}(555)$ inshore of 125°W (the cross-shore extent of the moored observations) show marked latitudinal differences between Washington and Oregon (Figure 1b). As expected from a relationship between low-salinity river plumes and light scattering (Pak et al., 1970; Palacios et al., 2009), good agreement is observed between the timing of $R_{rs}(555)$ peaks (Figure 1b) and total discharge (Figure 1a). The role of the Columbia River in advecting waters northward along the Washington coast in the first few months of the year, and to the south and outer edges of the OR shelf in the summer, is evident in the $R_{rs}(555)$ fields (Figures 1b and 2a,b). A secondary role for phytoplankton in contributing to increased $R_{rs}(555)$ signals in the summer cannot be disregarded. The cross-shore extent of the offshore advection of the plume during different times of the year is illustrated from glider observations (Figure 3), which reveal times when areas offshore of the OR line experience larger volumes of freshwater compared to the WA line as a result of Columbia River advection.

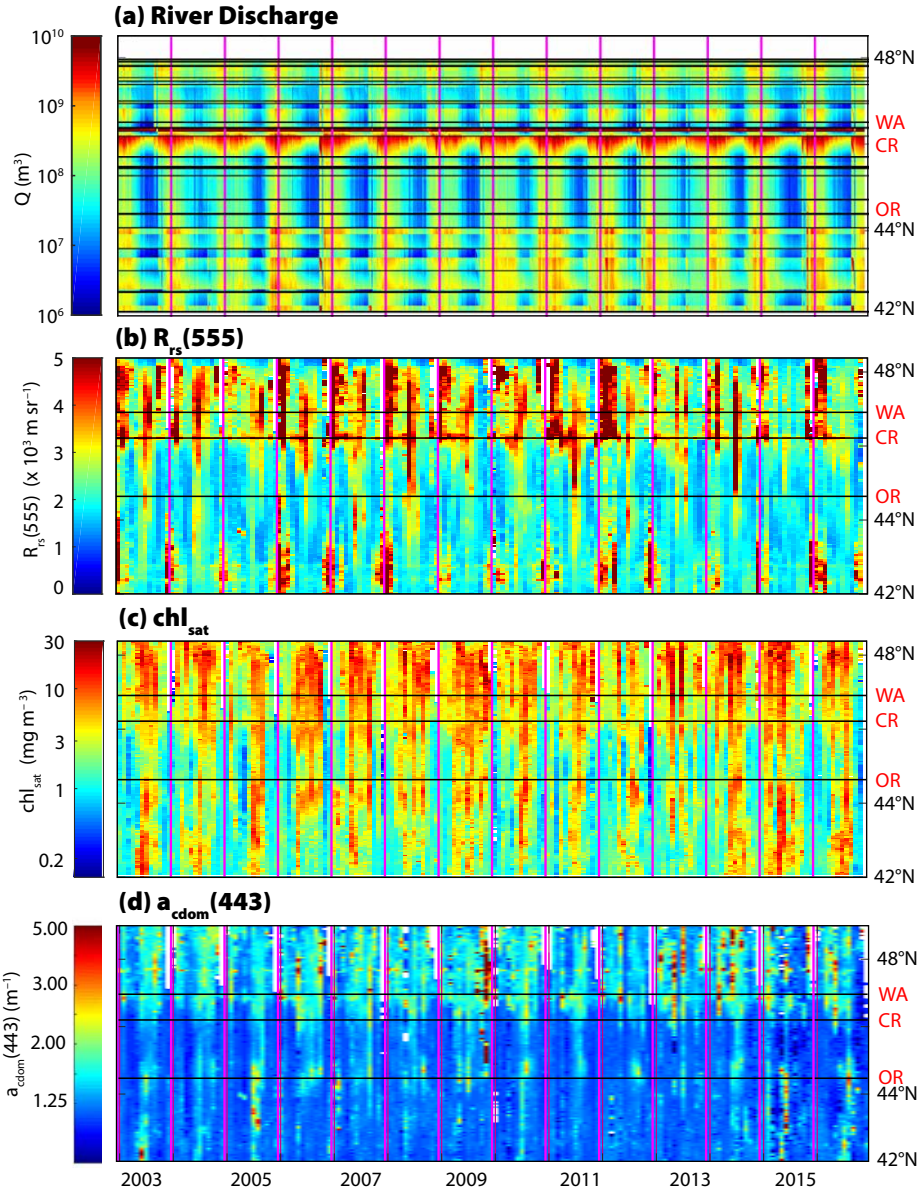

FIGURE 1. Hovmöller plot of (a) integrated monthly water discharge from US Geological Survey stations at the major rivers (horizontal black lines) along the Washington-Oregon coastline, including, from north to south, Calawah, Bogachiel, Hoh, Queets, Quinault, Wynoochee, Satsop, Chehalis, Willapa, Naselle, Columbia, Nehalem, Wilson, Trask, Nestucca, Siletz, Alsea, Siuslaw, Umpqua, South Fork Coquille, Rogue, and Chetco. The location of all river mouths is shown on the map to the right.. (b–d) remotely sensed estimates of (b) $R_{rs}(555)$, (c) chl_{sat}, and (d) $a_{cdom}(443)$ from the MODIS-Aqua sensor for coastal waters inshore of 125°W. Note that the discharge data are discrete measurements, and the interpolation along the latitude axis is for visualization purposes only. The vertical magenta lines correspond to January 1.

Discharge from mountainous coastal rivers as a result of high rainfall from "atmospheric rivers" of moisture (e.g., Warner et al., 2012), particularly to the south of the OR line, also correspond to increases in $R_{rs}(555)$ in winter months (Figure 1a,b). Nonetheless, the observed $R_{rs}(555)$ maxima inshore during fall/winter (Figure 2a,b) likely result from not only discharge patterns along the coast

but also increased particle resuspension processes following storm events, which in this region are marked by coherent changes in winds and surface wave heights (a proxy for mixing; Kniskern et al., 2011; see also Figure 6k–l). Indeed, long-period surface gravity waves have been shown to transport suspended sediments across the shelf and modulate changes in particulate backscattering (i.e., suspended materials) inshore of the 100 m isobath in the absence of strong riverine inputs (Drake and Cacchione, 1985; Henderikx Freitas et al., 2017). Notably, the distance between the coast and the 100 m isobath varies along the Washington–Oregon coastline (i.e., more than 35 km at and north of the WA line, ~32 km at the OR line due to the presence of the Stonewall Bank, and less than 15 km north and south of OR). These differences in shelf configuration may partially explain the overall lower $R_{rs}(555)$ values between 43°N and 46°N in Figure 1b, because offshore waters make up a larger portion of the area east of 125°W in some of those regions.

Temporal variability of chl_{sat} is also large (Figure 1c), with a higher magnitude and broader cross-shelf extent of chl_{sat} along the WA line compared to the OR line (Figure 2c,d). The coefficient of variation of the annual maximum of chl_{sat} at ~125°W of the OR and WA lines is 34% (range = 3.7–12.9 mg m^{-3}) and 70% (range = 8.5–56.8 mg m^{-3}), respectively. The maximum in chl_{sat} occurs between June and September at both locations, with OR showing a more distinct seasonal cycle than WA, where relatively high values of chl_{sat} appear to persist for longer periods during the upwelling season (Figure 2c,d). A matchup analysis between in situ chl observations from the OOI moorings and chl_{sat} estimates shows that the satellite data overestimate in situ chl observations closest to the coast (Figure 4a). This is because chl_{sat} algorithms rely on the use of information in the blue region of the reflectance spectrum, which in coastal areas is highly affected by the presence of absorbing aerosols, suspended sediments, and CDOM (Gordon, 1997; Dierssen, 2010). Satellite retrievals of $a_{cdom}(443)$ show overall larger signals in WA compared to OR (Figure 1d), and similar seasonal cycle patterns to those observed in chl_{sat} (Figure 2e,f). The enhanced cross-shore values in both chl_{sat} and $a_{cdom}(443)$ at WA during lower productivity months such as December (Figure 2e) are intriguing, and suggest a role for CDOM contamination in the chl_{sat} retrievals. The notion that phytoplankton, CDOM, and sediments all contribute to chl_{sat} signals implies that the seemingly high chl_{sat} concentrations at WA relative to OR may at least partially be a consequence of the proximity of WA to CDOM-rich sources such as the Columbia River plume and the Grays Harbor outflow (e.g., Palacios et al., 2009, 2012).

Cross-shore glider estimates of CDOM (Figure 3 and 5) suggest a stronger cross-shore gradient in CDOM concentrations off the WA shelf, even at times when larger volumes of freshwater are registered at the OR shelf (i.e., June 2016 in Figure 3o). Certainly, transport, dilution, and other biogeochemical processes that affect CDOM variability need to be considered when comparing distributions at the two sites. Additionally, the large bandwidth of the CDOM fluorometer is tuned to detect CDOM in turbid waters, and thus not suitable for examining subtle changes in this property in clearer ocean conditions further from the coast. Examples of well-resolved coastal glider observations in Figure 5 point to key differences between the cross-shore distribution of bio-optical properties at WA and OR. First, the differences in the bathymetry along the two Endurance Lines may explain the presence of bottom nepheloid layers at WA (as denoted by elevated b_{bp} and near zero chl values along the slope), which suggests that mixing processes may be more important to determining cross-shelf b_{bp} variability at WA than at OR (at least within the sampled region). Second, CDOM distributions over the shelf are notably different at the two locations (particularly in Figure 5b, where observations at the two locations were obtained simultaneously), with patterns in WA suggesting that the nearshore region acts as a source of CDOM. Additional data collected simultaneously along the WA and OR lines would be necessary to determine if these example features hold throughout different seasons and years.

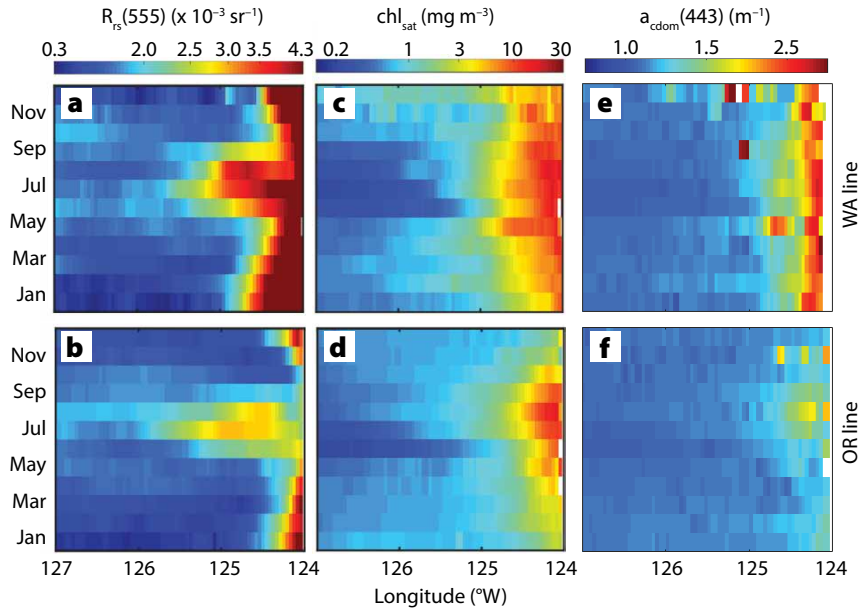

FIGURE 2. Annual mean of (a,b) $R_{rs}(555)$, (c,d) chl_{sat}, and (e,f) $a_{cdom}(443)$ along the Washington (top panels) and Oregon (bottom panels) Ocean Observatories Initiative Endurance Lines computed using MODIS observations for the 2003–2016 period. Note that $a_{cdom}(443)$ fails in very turbid coastal waters.

Latitudinal Gradients in Bio-Optical Properties from High-Frequency Moorings

High-frequency measurements from surface moorings expand the observations to the inner shelf regions of WA and OR, and provide temporally resolved observations that allow characterization of the latitudinal differences and interrelationships between bio-optical parameters over the 2015–2016 period (Figure 6). During the observed period, chl maxima at times occur at the mid-shelf sites rather than inshore, possibly following offshore advection of the upwelling front, whereas minima are generally found further from the coast (Figure 6a,b). In contrast, a more apparent cross-shore gradient is depicted in the b_{bp} observations, with elevated values generally occurring closest to shore (Figure 6c,d). Periods of synchronous changes in chl across the shelf are observed in a few instances (e.g., May and July 2016 at WA), but overall differences among the moorings denote the patchy nature of chl distributions across the shelf. The similarities and differences between chl and b_{bp} spatial and temporal distributions indicate variability in the types of materials dominating optical properties at the different moorings. Biogenic particles typical of productive pelagic oceanic environments have large chl and low-to-moderate b_{bp} values, whereas waters dominated by minerogenic particles have high b_{bp} and low chl concentrations (Henderikx Freitas et al., 2016). Thus, the relationships between b_{bp} and chl in Figure 4b for samples collected between May and September at both lines indicate that nearshore b_{bp} estimates are more likely

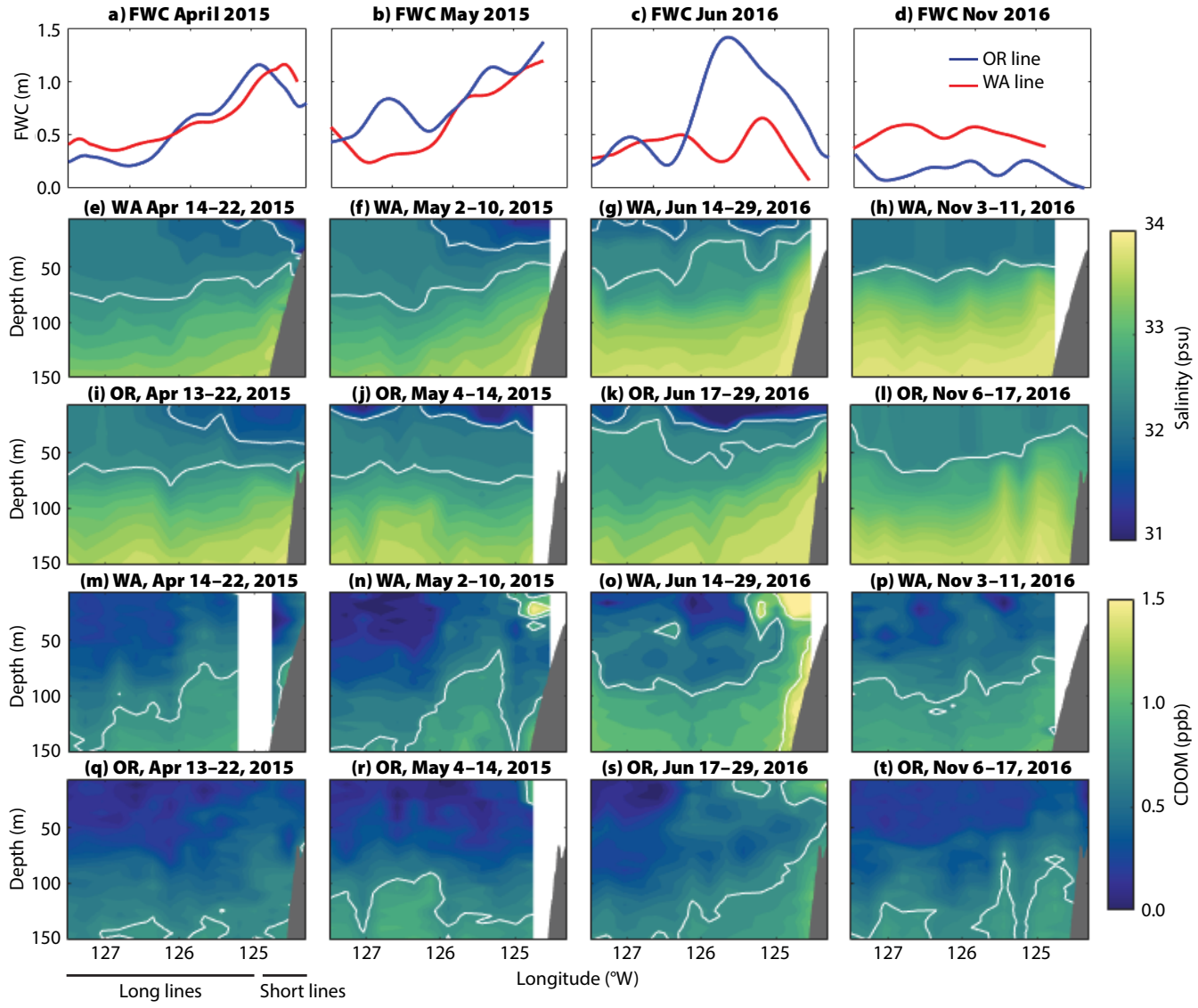

FIGURE 3. Cross-shore estimates of freshwater content, salinity, and chromophoric dissolved organic matter (CDOM) at the Washington (WA) and Oregon (OR) Endurance Lines from glider profiles for selected time periods during 2015 and 2016. Panels (a–d): the freshwater content (FWC) across the shelf; (e–l): cross-shore salinity profiles along the WA (e–h) and OR (i–l) lines where the white contours are the 32 and 32.5 psu isohalines; (m–t): cross-shore CDOM profiles along the WA (m–p) and OR (q–t) lines, where the white lines are the 0.75 and 1.25 ppb contours. Both long Endurance Line profiles (128°W to 125°W) and short Endurance Line profiles (125°W to 124.3°W) were used whenever available. Plots were made using smoothing lengths of 0.25 degrees (longitude) and 10 m (depth). White bars denote missing data.

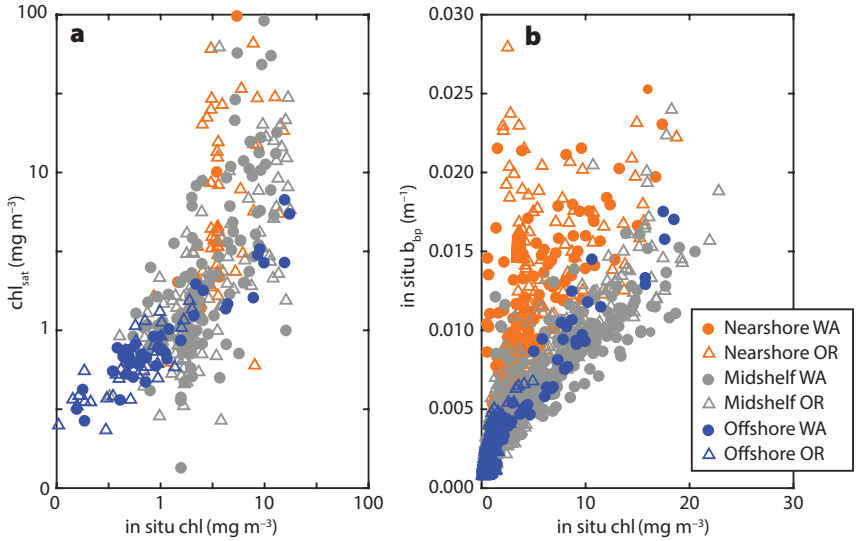

FIGURE 4. (a) Matchups between daily averages of in situ chl and chl$_{sat}$. Only the closest cloud-free pixel (4 km resolution) to each mooring was chosen for each available day whereas in situ chl were derived only from nighttime daily averages. Note that data availability due to cloud cover and QA/QC flags applied to satellite data led to variable matchup density between locations. (b) Correspondence between mooring optical measurements of b$_{bp}$ and chl for samples collected between May and September 2015 and 2016. Note that nearshore samples are more likely to show high b$_{bp}$ and low chl values, in agreement with characterization of non-phytoplankton particles.

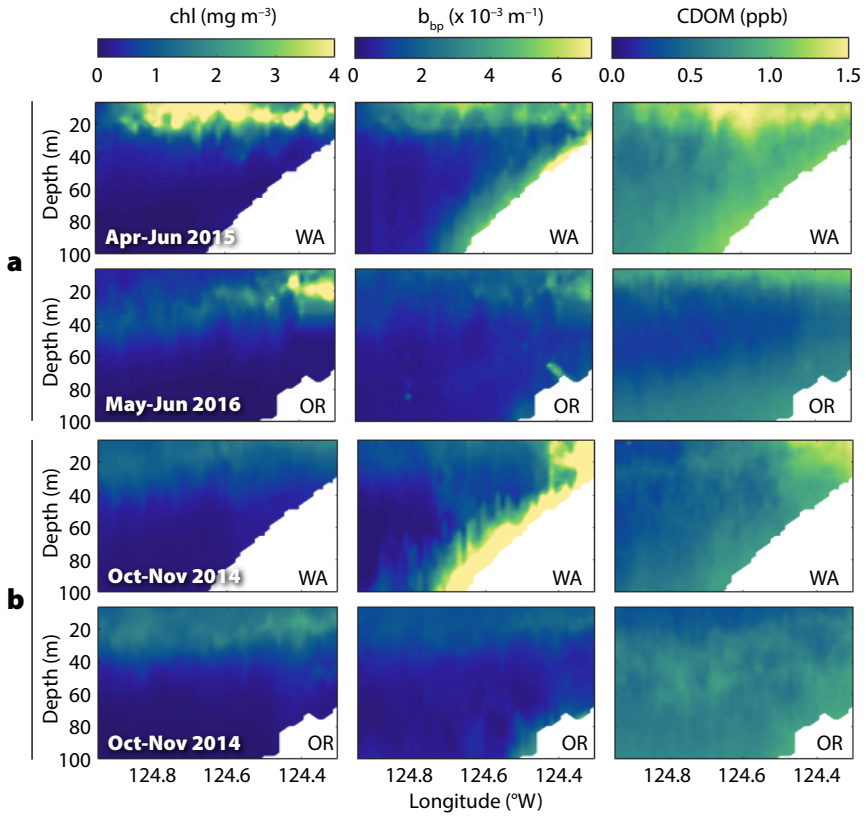

FIGURE 5. Examples of mean cross-shore sections of chl, b$_{bp}$, and CDOM for selected glider deployments along the WA and OR Endurance Lines. (a) Spring of 2015 (WA) and 2016 (OR). (b) Fall of 2014 for WA and OR. Ordinary krigging is used to plot the average quantities, with smoothing scales of 1 km (longitude) and 2 m (depth), and shallowest measurement of 6 m. Westernmost and easternmost longitudes are equivalent to the location of the offshore and mid-shelf moorings, respectively. Note that lack of coincident glider deployments in time largely prevented direct comparison between the two lines.

to be affected by non-phytoplankton materials (even in periods when discharge is presumably low), whereas optical properties of offshore samples are more likely to be dominated by changes in phytoplankton concentrations. These observations contextualize the relationships between chl and b$_{bp}$ with depth and distance from shore previously shown in the glider sections (Figure 5b).

The chl variations along the OR and WA lines are comparable over the course of the upwelling season, with mid-shelf averages of chl for the May–September months of 2015 and 2016 reaching 3.34 ± 2.58 (one standard deviation) mg m^{-3} at WA and 4.61 ± 2.65 mg m^{-3} at OR. However, differences between OR and WA chl concentrations can exceed 20 mg m^{-3} at any given time during the more productive months of the years (e.g., August 2016; Figure 6a,b). Nonetheless, these values are considerably different from the average seasonal concentrations suggested from satellite estimates (Figures 1c and 2c,d). Nearshore b$_{bp}$ patterns at WA and OR are also comparable in timing and magnitude, but differences are apparent in the mid-shelf, where WA waters show elevated backscattering compared to OR in the winter months (Figure 6c,d). The similarities nearshore are expected because both WA and OR are under the influence of riverine inputs, but mid-shelf differences may point to the broader cross-shore extent of the Columbia River plume off WA compared to coastal river plumes created by smaller rivers to the south off OR. Bathymetry differences between the two lines may also explain these mid-shelf discrepancies, as illustrated from glider observations (Figure 5). The temporal distribution of CDOM somewhat agrees with that of b$_{bp}$ when concentrations are high, particularly during winter, whereas during the remaining periods values oscillate above a background that is larger at WA during 2015, and relatively similar at WA and OR in 2016 (Figure 6e,f). The consistently lower CDOM concentrations at the mid-shelf OR mooring compared to offshore OR between October 2015 and March 2016 (Figure 6f) are suspicious, and may indicate drift or instrument issues.

In contrast with the optical properties, consistent cross-shore gradients in temperature

are observed across WA and OR, with nearshore waters presenting the coolest overall observations. Cross-shore gradients in temperature are strongest in spring-summer, consistent with the expected effects of upwelling and solar heating, and less pronounced in fall-winter, following stronger mixing processes. Nearshore and mid-shelf temperatures are overall cooler during the upwelling season in OR, as expected given the stronger wind conditions in OR compared to WA (wind stress is on average 1.5 times stronger on the Oregon shelf compared to the Washington shelf during the 2015–2016 period; Figure 6l). Salinity patterns in OR present marked seasonal changes in nearshore values (Figure 6i), showing the most saline waters in spring-summer and the freshest values in fall-winter. Salinity values are freshest overall along the WA line, as expected given its proximity to the Columbia River (Figure 6j). Low-salinity peaks in December 2015 and January 2016 at both WA and OR inshore moorings (Figure 6i,j) agree well with CDOM maxima in Figure 6e,f. It is important to note that although the surface mooring observations cannot vertically resolve variations of physical and bio-optical properties, surface chl values have been shown to be well correlated with depth-integrated chl at the OR line (McKibben, 2016). However, we cannot exclude the importance of subsurface features such as thin layers of phytoplankton or bottom and intermediate nepheloid layers that are not sampled by the moorings (e.g., Figure 5). Additionally, the role of upwelling in lifting isopycnals toward the coast (and therefore changing the vertical distribution of chl across the shore) as suggested between May and June 2016 in OR (Figure 5a), undoubtedly complicates interpretation of moored data that are measured at the same depth (7 m) across the shelf. Further analyses should be expanded to include OOI Profiler Mooring data in order to resolve these vertical variations. Concurrent profiler data, however, were not available for the time period of this study.

Processes Controlling Observed Variability in In Situ Optical Properties

Establishing causal links between physical and biogeochemical changes in the surface ocean is not trivial. Cumulative alongshore wind stress, a metric that represents energy input into the upwelling system over the course of each season, is plotted in Figure 7 for WA and OR for periods of 2015 and 2016. Cumulative chlorophyll values over time, which are commonly used to assess bloom initiation times (e.g., Brody et al., 2013) and to summarize and highlight major changes in local chl values (e.g., McQuatters-Gollop et al., 2008), are also plotted in Figure 7 as cumulative chl anomaly relative to the respective time-series minimum (e.g.,, rapid and large increases in chl lead to increasing slopes, and small or null changes lead to flat slopes). The importance of upwelling events in driving increases in mid-shelf chl is clear at both locations, as abrupt increases in cumulative wind stress quantities are generally accompanied by steeper slopes of cumulative chl values (e.g., June 2015 and July–August 2016). In contrast, periods of flat or negative cumulative wind stress slopes (e.g., July 2015 for both WA and OR and

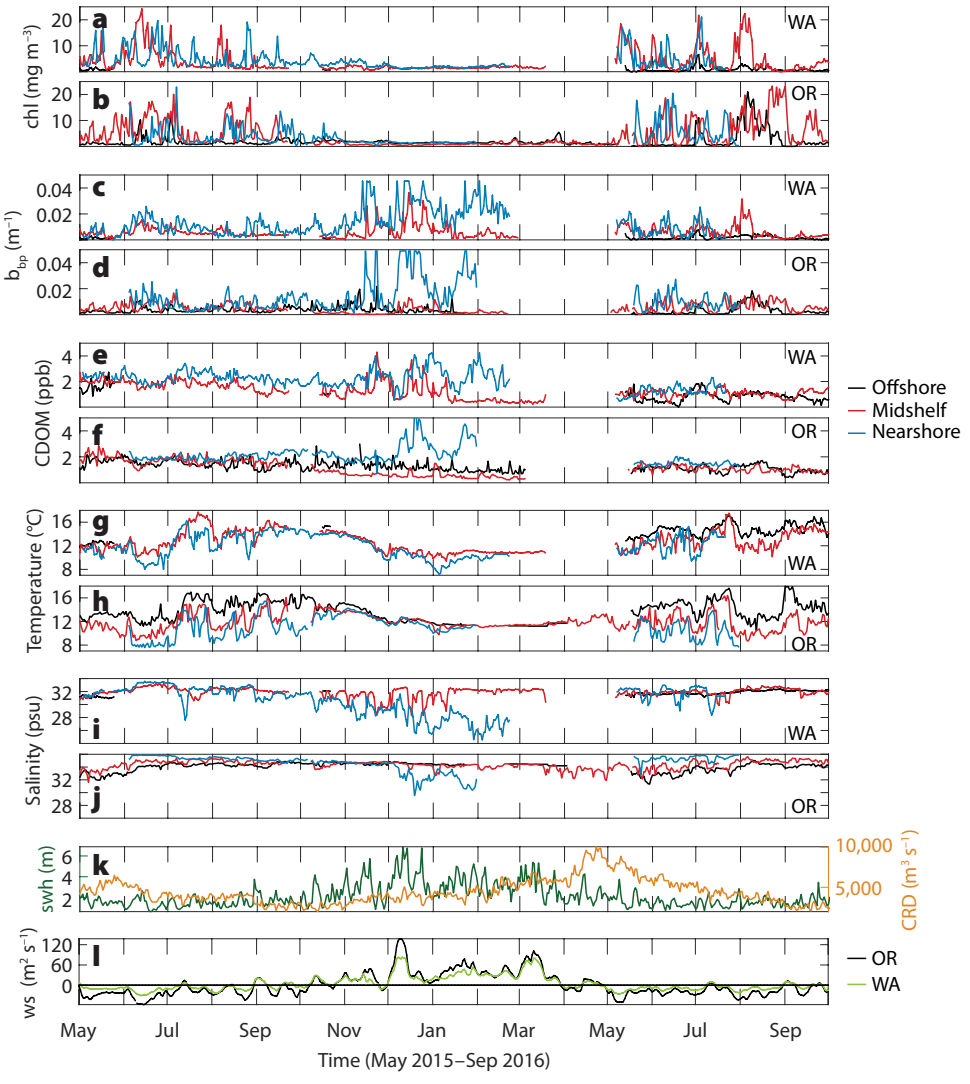

FIGURE 6. Temporal evolution of physical and optical variables at 7 m depth across the moorings of the WA and OR Endurance Lines (from daily averages). swh = significant wave height from the National Data Buoy Center (NDBC) buoy 46041. CRD = Columbia River Discharge. ws = alongshore wind stress convoluted with eight-day exponential decay as in Austin and Barth (2002). Wind stress measurements are from NDBC buoys 46041 (WA) and 46050 (OR). SWH at WA and OR buoys are well correlated with an $r^2 = 0.90$ for the 2005–2016 period.

August–September 2016 for WA) show overall flat cumulative chl anomalies. The late summer increases in cumulative chl in OR compared to WA during both years analyzed (also apparent in Figure 6a,b) may be related to the longer duration of the upwelling season at OR compared to WA. Nonetheless, the elevated chl values at WA despite much weaker upwelling-favorable winds indicate that other processes must contribute to the chl signals off WA, as reported by previous authors (e.g., Hickey and Banas, 2008). However, the latitudinal differences between chl estimates at WA and OR may not be as strong as the differences suggested from satellite data, given the relative similarity in the timing and magnitude of the variability of in situ chl estimates at the two lines (Figures 6a,b and 7). Although the moored observations alone are not sufficient to assess whether the apparent similarities in chl distribution (and the observed higher chl concentrations in OR in the summer) hold over multiple seasons and years, we hypothesize based on the evidence presented here that CDOM may be an important factor affecting the latitudinal differences observed from satellite-derived chl estimates (Figure 2). This is particularly relevant when interpreting chl_{sat} signals off the Washington coastline, given the strong interference of the CDOM-rich Columbia River plume at those locations (Palacios et al., 2009, 2012).

The OOI b_{bp} record shows the importance of biological land-ocean interactions and resuspension processes in controlling b_{bp} distributions. Salinity and b_{bp} are inversely correlated at all WA moorings (r = −0.16, −0.33, and −0.53 offshore, at the mid-shelf, and inshore, respectively) and at the inshore OR mooring (r = −0.57). This indicates that allochthonous sources partially control b_{bp} variability particularly at the inshore moorings. However, positive (but weak) correlations are observed at the mid-shelf and offshore OR moorings (r = 0.29 and r = 0.21, respectively), indicating the added importance of pelagic phytoplankton in characterizing the bulk b_{bp} further offshore at OR, as shown in Figure 4b. Evidence for the role of mixing or resuspension processes in affecting the variability in b_{bp} is observed between November 2015 and January 2016, when increases in nearshore b_{bp} at WA and OR occur during a period of downwelling-favorable winds (Figure 6l), increased significant surface wave height conditions, and relatively low discharge (Figure 6k). Indeed, positive relationships are observed between b_{bp} and significant wave heights at the WA and OR inshore moorings (r = 0.61 and r = 0.51, respectively; correlations are the strongest at zero lag), whereas the relationships with discharge are weaker at the OR inshore mooring (r = 0.16), and, surprisingly, not significant at WA. The lack of strong relationships with discharge may be related to the relatively low discharge levels observed in 2015 compared to the climatology (see Figure 1). Nonetheless, these observations indicate that river discharge alone does not explain nearshore particle distributions. No significant correlations are observed between wave heights and b_{bp} at any of the mid-shelf or offshore moorings, as expected given the constraint that increased depths impose on the particle resuspension processes.

CONCLUSIONS

Satellite observations of chl along the Washington-Oregon latitudinal range are consistent with the existing paradigm of higher annual magnitude and larger cross-shore extent of chl signals off the Washington shelf, despite reduced upwelling strength compared to Oregon. However, in situ bio-optical data for the time period of OOI data availability show relative similarity between the magnitude of the cross-shore chl distributions at WA and OR, and increased presence of suspended sediments and CDOM off WA. These observations, although temporally limited, indicate potential contamination of satellite retrievals of chl due to CDOM and suspended materials in the water column, particularly off the WA shelf, that should caution further attribution of chl_{sat} signals to differences in production. Nonetheless, the considerable differences in wind stress between WA and OR indicate that processes other than upwelling are important for determining chl distributions at WA, as previously suggested. Glider-derived data show the strong seasonal influence of the Columbia River plume as a source of freshwater to the shelf off WA and to OR offshore waters, in agreement with known shifts in wind forcing. Full water column depth analysis using profiler and additional glider data that temporally align with each other and with mooring data during key seasonal events would be needed to ascribe latitudinal gradients in chl and particle distributions to variations in productivity.

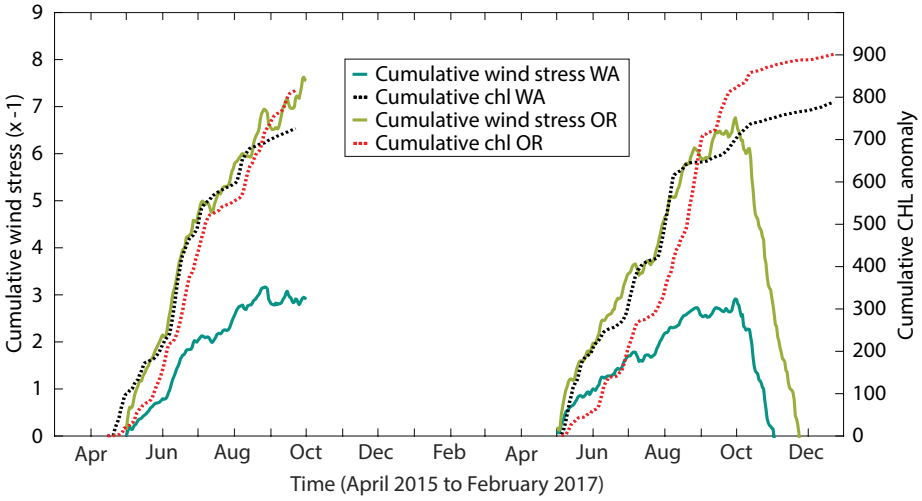

FIGURE 7. Cumulative wind stress and cumulative chl anomalies for mid-shelf observations at WA and OR moorings for mid-April to September 2015 and May to December 2016.

As the OOI time series matures, we will be better poised to discriminate between riverine impacts on particle loading and plankton productivity, and to more conclusively address the factors that lead to biogenic carbon production and export in the Northern California Current ecosystem.

REFERENCES

Austin, J.A., and J.A. Barth. 2002. Variation in the position of the upwelling front on the Oregon shelf. *Journal of Geophysical Research* 107(C11), 3180, https://doi.org/10.1029/2001JC000858.

Barnes, C.A., A.C. Duxbury, and B. Morse. 1972. Circulation and selected properties of the Columbia River effluent at sea. Pp. 71–80 in *The Columbia River Estuary and Adjacent Ocean Waters: Bioenvironmental Studies*. A.T. Pruter and D.L. Alveison, eds, University of Washington Press, Seattle.

Brody, S.R., M.S. Lozier, and J.P. Dunne. 2013. A comparison of methods to determine phytoplankton bloom initiation. *Journal of Geophysical Research* 118(5):2,345–2,357, https://doi.org/10.1002/jgrc.20167.

Coble, P.G. 1996. Characterization of marine and terrestrial DOM in seawater using excitation-emission matrix spectroscopy. *Marine Chemistry* 51(4):325–346, https://doi.org/10.1016/0304-4203(95)00062-3.

Cullen, J.J. 1982. The deep chlorophyll maximum: Comparing vertical profiles of chlorophyll *a*. *Canadian Journal of Fisheries and Aquatic Sciences* 39:791–803, https://doi.org/10.1139/f82-108.

Davis, K.A., N.S. Banas, S.N. Giddings, S.A. Siedlecki, P. MacCready, E.J. Lessard, R.M. Kudela, and B.M. Hickey. 2014. Estuary-enhanced upwelling of marine nutrients fuels coastal productivity in the US Pacific Northwest. *Journal of Geophysical Research* 119:8,778–8,799, https://doi.org/10.1002/2014JC010248.

Dickson, M., and P.A. Wheeler. 1995. Nitrate uptake rates in a coastal upwelling regime: A comparison of PN-specific, absolute, and Chl a-specific rates. *Limnology and Oceanography* 40, https://doi.org/10.4319/lo.1995.40.3.0533.

Dierssen, H.M. 2010. Perspectives on empirical approaches for ocean color remote sensing of chlorophyll in a changing climate. *Proceedings of the National Academy of Sciences of the United States of America* 107:17,073–17,078, https://doi.org/10.1073/pnas.0913800107.

Drake, D.E., and D.A. Cacchione. 1985. Seasonal variation in sediment transport on the Russian River Shelf, California. *Continental Shelf Research* 4:495–514, https://doi.org/10.1016/0278-4343(85)90007-X.

Goñi, M.A., J.A. Hatten, R.A. Wheatcroft, and J.C. Borgeld. 2013. Particulate organic matter export by two contrasting small mountainous rivers from the Pacific Northwest, USA. *Journal of Geophysical Research* 118:112–134, https://doi.org/10.1002/jgrg.20024.

Gordon, H.R. 1997. Atmospheric correction of ocean color imagery in the Earth Observing System era. *Journal of Geophysical Research* 102(D14):17,081–17,106, https://doi.org/10.1029/96JD02443.

Henderikx Freitas, F., D.A. Siegel, S. Maritorena, and E. Fields. 2017. Satellite assessment of particulate matter and phytoplankton variations in the Santa Barbara Channel and its surrounding waters: Role of surface waves. *Journal of Geophysical Research* 122:355–371, https://doi.org/10.1002/2016JC012152.

Henderikx Freitas, F., D.A. Siegel, L. Washburn, S. Halewood, and E. Stassinos. 2016. Assessing controls on cross-shelf phytoplankton and suspended particle distributions using repeated bio-optical glider surveys. *Journal of Geophysical Research* 121:7,776–7,794, https://doi.org/10.1002/2016JC011781.

Hickey, B.M., and N.S. Banas. 2003. Oceanography of the US Pacific Northwest coastal ocean and estuaries with application to coastal ecology. *Estuaries* 26(4):1,010–1,031, https://doi.org/10.1007/BF02803360.

Hickey, B.M., and N.S. Banas. 2008. Why is the northern end of the California Current System so productive? *Oceanography* 21(4):90–107, https://doi.org/10.5670/oceanog.2008.07.

Hickey, B.M., S. Geier, N. Kachel, and A. Macfadyen. 2005. A bi-directional river plume: The Columbia in summer. *Continental Shelf Research* 25:1,631–1,656, https://doi.org/10.1016/j.csr.2005.04.010.

Hickey, B.M., L.J. Pietrafesa, D.A. Jay, and W.C. Boicourt. 1998. The Columbia River plume study: Subtidal variability in the velocity and salinity fields. *Journal of Geophysical Research* 103(C5):10,339–10,368, https://doi.org/10.1029/97JC03290.

Huyer, A. 1983. Coastal upwelling in the California Current system. *Progress in Oceanography* 12(3):259–284, https://doi.org/10.1016/0079-6611(83)90010-1.

Jonasz, M., and G. Fournier. 2011. *Light Scattering by Particles in Water: Theoretical and Experimental Foundations.* Academic Press, 704 pp.

Kniskern, T.A., J.A. Warrick, K.L. Farnsworth, R.A. Wheatcroft, and M.A Goñi. 2011. Coherence of river and ocean conditions along the US West Coast during storms. *Continental Shelf Research* 31(7):789–805, https://doi.org/10.1016/j.csr.2011.01.012.

Maritorena, S., D.A. Siegel, and A.R. Peterson. 2002. Optimization of a semianalytical ocean color model for global-scale applications. *Applied Optics* 41(15):2,705–2,714, https://doi.org/10.1364/AO.41.002705.

McKibben, S.M. 2016. *Above and Below: Oregon Coastal Phytoplankton Bloom Dynamics from Sea and Space*. PhD Thesis, Oregon State University, Corvallis, Oregon.

McQuatters-Gollop, A., L.D. Mee, D.E. Raitsos, and G.I. Shapiro. 2008. Non-linearities, regime shifts and recovery: The recent influence of climate on Black Sea chlorophyll. *Journal of Marine Systems* 74(1):649–658, https://doi.org/10.1016/j.jmarsys.2008.06.002.

Müller, P., X.-P. Li, and K.K. Niyogi. 2001. Non-photochemical quenching: A response to excess light energy. *Plant Physiology* 125(4):1,558–1,566, https://doi.org/10.1104/pp.125.4.1558.

Palacios, S.L., T.D. Peterson, and R.M. Kudela. 2009. Development of synthetic salinity from remote sensing for the Columbia River plume. *Journal of Geophysical Research* 114, C00B05, https://doi.org/10.1029/2008JC004895

Palacios, S.L., T.D. Peterson, and R.M. Kudela. 2012. Optical characterization of water masses within the Columbia River plume. *Journal of Geophysical Research* 117, C11020, https://doi.org/10.1029/2012JC008005.

Pak, H., G.F. Beardsley Jr., and P.K. Park. 1970. The Columbia River as a source of marine light-scattering particles. *Journal of Geophysical Research* 75(24):4,570–4,578, https://doi.org/10.1029/JC075i024p04570

Saldías, G.S., R.K. Shearman, J.A. Barth, and N. Tufillaro. 2016. Optics of the offshore Columbia River plume from glider observations and satellite imagery. *Journal of Geophysical Research* 121:2,367–2,384, https://doi.org/10.1002/2015JC011431.

Schmechtig, C., H. Claustre, A. Poteau, and F. D'Ortenzio. 2014. *Bio-Argo Quality Control Manual for the Chlorophyll-A Concentration*, Version 1.0. Ifremer, 16 pp., https://doi.org/10.13155/35385.

Smith, L.M., J.A. Barth, D.S. Kelley, A. Plueddemann, I. Rodero, G.A. Ulses, M.F. Vardaro, and R. Weller. 2018. The Ocean Observatories Initiative. *Oceanography* 31(1):16–35, https://doi.org/10.5670/oceanog.2018.105.

Sullivan, J.M. 2013. Measuring optical backscattering in water. Pp. 189–224 in *Light Scattering Reviews 7: Radiative Transfer and Optical Properties of Atmosphere and Underlying Surface.* J.M. Sullivan, M.S. Twardowski, J.R.V. Zaneveld, C.C. Moore, and A. Kokhanovsky, eds, Praxis Publishing Ltd.

Thomas, A.C., and R.A. Weatherbee. 2006. Satellite-measured temporal variability of the Columbia River plume. *Remote Sensing of Environment* 100:167–178, https://doi.org/10.1016/j.rse.2005.10.018.

Ware, D.M., and R.E. Thomson. 2005. Bottom-up ecosystem trophic dynamics determine fish production in the Northeast Pacific. *Science* 308(5726):1,280–1,284, https://doi.org/10.1126/science.1109049.

Warner, M.D., C.F. Mass, and E.P. Salathé. 2012. Wintertime extreme precipitation events along the Pacific Northwest coast: Climatology and synoptic evolution. *Monthly Weather Review* 140:2,021–2,043, https://doi.org/10.1175/MWR-D-11-00197.1.

Wetz, M.S., and P.A. Wheeler. 2003. Production and partitioning of organic matter during simulated phytoplankton blooms. *Limnology and Oceanography* 5, https://doi.org/10.4319/lo.2003.48.5.1808.

Wheatcroft, R.A., M.A. Goñi, J.A. Hatten, G.B. Pasternack, and J.A. Warrick. 2010. The role of effective discharge in the ocean delivery of particulate organic carbon by small, mountainous river systems. *Limnology and Oceanography* 55:161–171, https://doi.org/10.4319/lo.2010.55.1.0161.

Zhang, X., L. Hu, and M.-X. He. 2009. Scattering by pure seawater: Effect of salinity. *Optics Express* 17(7):5,698–5,710, https://doi.org/10.1364/OE.17.005698.

ACKNOWLEDGMENTS

This work was funded by the National Science Foundation (OCE-1642295 to MG, AW, KS) with additional support from the Simons Foundation via the SCOPE program (AW). All matlab code for data processing and generation of figures are available upon request to the corresponding author (awhite@coas.oregonstate.edu). We are particularly grateful to Stuart Pearce at OOI for access to the glider data streams.

AUTHORS

Fernanda Henderikx Freitas is Research Associate, College of Earth, Ocean, and Atmospheric Sciences (CEOAS), Oregon State University, Corvallis, OR, USA. **Gonzalo S. Saldías** completed his PhD at CEOAS, Oregon State University, Corvallis, OR, USA, and is currently a researcher at Centro FONDAP de Investigación en Dinámica de Ecosistemas Marinos de Altas Latitudes (IDEAL), Valdivia, Chile. **Miguel Goñi** is Professor, **R. Kipp Shearman** is Associate Professor, and **Angelicque E. White** (awhite@coas.oregonstate.edu) is Associate Professor, all at CEOAS, Oregon State University, Corvallis, OR, USA.

ARTICLE CITATION

Henderikx Freitas, F., G.S. Saldías, M. Goñi, R.K. Shearman, and A.E. White. 2018. Temporal and spatial dynamics of physical and biological properties along the Endurance Array of the California Current ecosystem. *Oceanography* 31(1):80–89, https://doi.org/10.5670/oceanog.2018.113.